Arch. Metall. Mater. **64** (2019), 2, 613-616

DOI: 10.24425/amm.2019.127587

MIN CHUL OH*†, HYUNJOO SEOK*†, YEONGCHEOL JO**, BYUNGMIN AHN*#

NOVEL TECHNIQUE TO PRODUCE HYBRID P/M COMPONENTS USING DISSIMILAR FERROUS ALLOYS

The objective of the present research is to develop the novel multi-compaction technology to produce hybrid structure in powder metallurgy (P/M) components using dissimilar Fe-based alloys. Two distinct powder alloys with different compositions were are used in this study: Fe-Cr-Mo-C pre-alloyed powder for high strength and Fe-Cu-C mixed powder for enhanced machinability and lower material cost. Initially, Fe-Cu-C was pre-compacted using a bar-shaped die with lower compaction pressure. The green compact of Fe-Cu-C alloy was inserted into a die residing a half of the die, and another half of the die was filled with the Fe-Cr-Mo-C powder. Then they subsequently underwent re-compaction with higher pressure. The final compact was sintered at 1120°C for 60 min. In order to determine the mechanical behavior, transverse rupture strength (TRS) and Vickers hardness of sintered materials were measured and correlated with density variations. The microstructure was characterized using optical microscope and scanning electron microscope to investigate the interfacial characteristics between dissimilar P/M alloys.

Keywords: Hybrid Fe alloy, Multi-compaction, Interface boundary, Diffusion behavior

1. Introduction

Pre-alloyed high-alloy Fe powder is commonly used for enhancing strength in various P/M products in commercial manufacturing sectors [1-5]. However, P/M components made of high-alloy Fe powder are generally expensive because of high raw material cost, and exhibit low machinability compared with those made of low-alloy Fe powder [6-8]. For optimum combination between performance, cost, and machinability, the development of hybrid structured P/M products is beginning to receive attention. The demand of hybrid structured P/M parts has been increased for various applications from parts of small electronic devices to parts of heavy engines and components. The main concept of hybrid structure using dissimilar alloys in this study is to use both high-alloy Fe powder where high strength and stiffness is required and low-alloy Fe powder where excellent machinability is required. Previously, there have been many attempts to make hybrid structures using dissimilar alloys. However, most research has been done on the multiple layered structure which can be performed easily feeding one alloy powder first and subsequently another one later. This technique requires only one compaction process after feeding. In the present study, the hybrid structure is achieved by locating dissimilar alloy powders side-by-side or inside-outside which may require more than one compaction step. Due to its complexity of the compaction processes which can cause inhomogeneous density distribution, an in-depth understanding of compaction conditions is necessary. The main objective of this research is to examine the feasibility of the multi-compaction method to produce hybrid P/M components which consists of dissimilar alloys inside-and-outside of cylindrical specimens. The effect of compacting pressure and the behavior at interfacial boundary between dissimilar alloys were investigated in detail.

2. Experimental

The high-alloy (Fe-Cr-Mo-C) powder was prepared with the mixing of Astaloy® CrM® powders (water-atomized Fe powder pre-alloyed with 3.0 wt.% Cr and 0.5 wt.% Mo manufactured and supplied by the Höganäs, Sweden) with addition of 0.5 wt.% C. The addition of Cr and Mo in Fe powder are well known for improving mechanical properties. Cr is mostly known as a stabilizer of ferrite with high tendency to combine with C in Fe powder forming chromium carbides and to suppress grain growth at sintering and heating processes. Mo in Fe powder is also acting as a ferrite stabilizer and leads to solid solution hardening forming bainite at quenching process. The low-alloy powder was prepared with the mixing of Fe, 3 wt.% Cu, and 0.5 wt.% C. The mixing process for both high- and low-alloys was performed using 3-D Tubular mixer for 60 min with addition of 0.5 wt.% of solid lubricant.

* AJOU UNIVERSITY, DEPARTMENT OF MATERIALS SCIENCE AND ENGINEERING AND DEPARTMENT OF ENERGY SYSTEMS RESEARCH, SUWON, GYEONGGI, 16499, KOREA
** CORPORATE RESEARCH & DEVELOPMENT DIVISION, HYUNDAI MOTOR COMPANY & KIA MOTORS CORPORATION, HWASEONG, GYEONGGI, 18280, KOREA

† These authors contributed equally to this work.

Corresponding author: byungmin@ajou.ac.kr

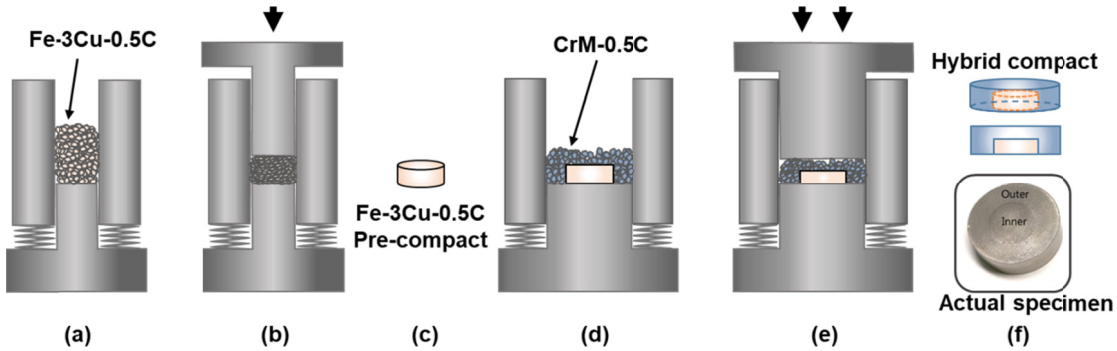

Fig. 1. A schematic illustration of compaction steps for hybrid structure using dissimilar ferrous alloys

To fabricate the hybrid structure using two dissimilar ferrous powders, modified version of compacting process is newly proposed in this research consisting of (i) feeding low-alloy powder, (ii) primary compaction of low-alloy powder, (iii) secondary feeding high-alloy powder around the low-alloy compact, and (iv) secondary compaction of all, as illustrated in Fig. 1. The primary compaction of low-alloy powder was performed using 1.27 mm diameter die with a pressure of 200 MPa which is just suitable to maintain the shape of green body. The secondary compaction of hybrid structure was performed using 2.54 mm diameter die with three different pressures of 500, 600, and 700 MPa.

After the compaction, specimens were de-lubricated at 700°C for 30 min and sintered at 1120°C for 60 min in N_2-$20H_2$ atmosphere in a rate of 10°C/min. Finally, the specimens were cooled in furnace at room temperature. The hardness was measured using nano-indenter, and the microstructure was investigated by optical microscope (OM) and scanning electron microscope (SEM) equipped with energy dispersive spectroscopy (EDS).

3. Results and discussion

Figure 2 shows both green and sintered relative densities of the hybrid compacts depending on the secondary compaction pressures. Because the primary compaction pressure was relatively low (200 MPa) which is just suitable to maintain the shape of green bodies, further densification can be achieved by the secondary compaction. Also, both green and sintered density increases as the secondary compaction pressure increases. A noticeable point in this density varication is that the sintered densities were even higher than green densities for all cases of three secondary compaction pressures. The Cu is an element which is generally melted and expands its volume during sintering of Fe-based P/M alloy, called as liquid-phase sintering [9-10]. Therefore, Cu addition in Fe-based P/M alloy generally gives rise to decrease in sintered density [11-14]. However, in the present study, the density of hybrid structure was increased after sintering. In the high-alloy part, pores can be effectively eliminated by solid-phase sintering compared with liquid-phase sintering in the low-alloy part. Also, this hybrid structure consists of the low-alloyed (Fe-3Cu-0.5C) inner core about 13 vol. % and the high-alloyed (CrM-0.5C) outer rim about 87 vol. %. Therefore, because the densification effect in the high-alloy part is more dominant over density decrease in the low-alloy part, the sintered density of hybrid structure increase in spite of the presence of Cu element.

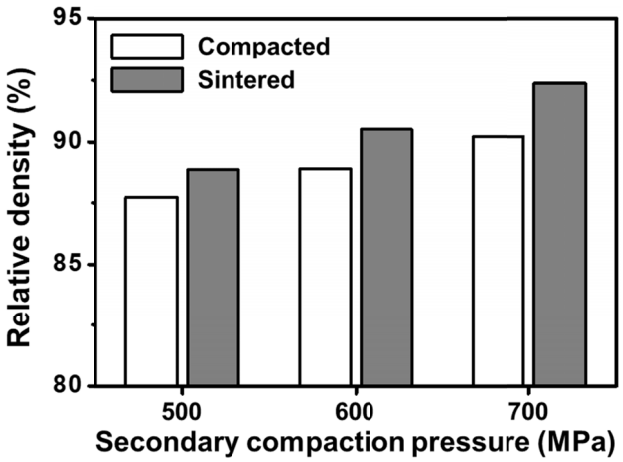

Fig. 2. As-compacted and as-sintered relative densities of hybrid structure depending on the secondary compaction pressure

Figure 3 exhibits un-etched optical micrographs of the interfacial region in hybrid structure. In both Fig. 3(a) and 3(b), the interface is located at the central part of the micrographs, and high- and low-alloy regions are in the left- and right-side of interface, respectively. When the hybrid structure was secondarily compacted with relatively lower pressure (500 MPa) in Fig. 3(a), a large amount of pores exists in both regions. In the high-alloy region, the CrM alloy powder generally exhibits low compactability due to its higher strength [15-16] so that at lower compaction pressure (500 MPa) a large amount of pores remained. However, at higher compaction pressure (700 MPa), the plastic deformation of high strength CrM alloy powder occurred so that the contact area between powder particles increased which assists elimination of pores. In the low-alloy region, although the low-alloy part was primarily compacted before the high-alloy powder was fed and underwent compaction twice, there are still significant amount of pore remained in Fig. 3(a). When it was secondarily compacted with higher pressure (700 MPa) in Fig. 3(b), most of large pores were elimi-

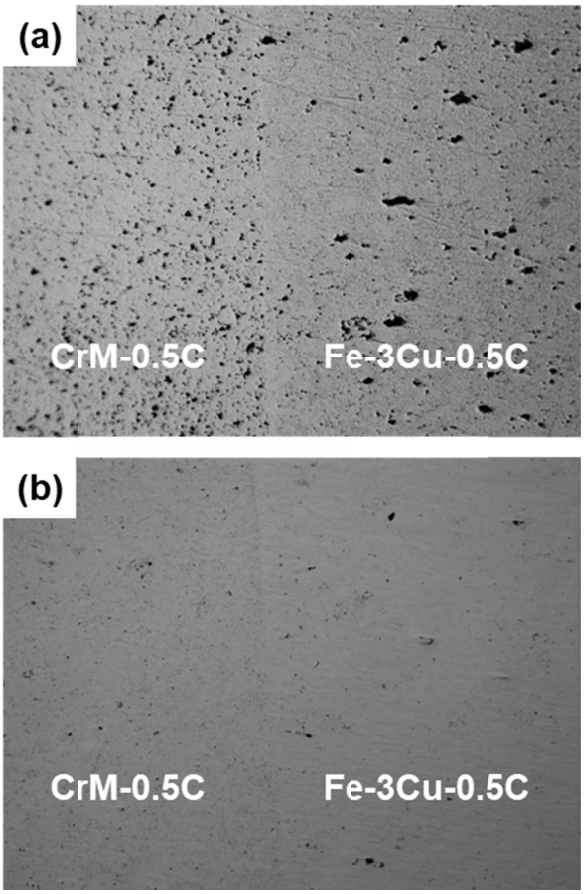

Fig. 3. Un-etched micrographs of interfacial region between high- and low-alloys when secondarily compacted with (a) 500 MPa and (b) 700 MPa

nated although a small pores remained which stemmed from the expansion and contraction of the Cu element during sintering process. This also implies that, in terms of pore removal, there is a critical compaction pressure to achieve a certain relative density regardless of number of compaction strike for both high- and low-alloys. In addition, no noticeable interfacial boundary was observed in both Fig. 3(a) and 3(b) indicating that there was no cracks or significant defects at the interface.

As-shown in Fig. 4(a), the mechanical property of the hybrid specimens was measured using nano-indentation hardness according to the secondary compaction pressure. The X-axis in Fig. 4(a) represents the relative location in the hybrid structure. Figure 4(b) and 4(c) show scanning electron micrographs of high- and low-alloy regions, respectively. As expected, the high-alloy (CrM-0.5C) region exhibits greatest hardness among three regions regardless of the secondary compaction pressure. In this region, the pre-alloyed Cr reacts with C during sintering and forms Cr carbides [17-19]. The Cr carbides inhibit the diffusion of C resulting in the formation of pearlite with fine lamella spacing as shown in Fig. 4(b). The mechanical property of cementite is improved as the fraction of cementite increased and as the cementite lamella spacing became smaller [18-20]. However, the low-alloy (Fe-3Cu-0.5C) part exhibits lowest hardness among three regions, because Cu in the Fe-Cu-C powder acts as a ferrite-stabilizing element which increases the fraction of coarse ferrite during sintering forming micro-pores as shown in Fig. 4(c). The interfacial region exhibits intermediate hardness between the high-alloy and low-alloy regions. This implies that there was no cracks or large pores exist in the interface between high- and low-alloys which affects decrease of hardness. Therefore, it can be expected that the transition between high- and low-alloy regions was smooth.

Also, the hardness increases in all three regions as the secondary compaction pressure increases as shown in Fig. 4(a). The effect of the secondary compaction pressure is more pronounced in the mixed low-alloy (Fe-3Cu-0.5C) region compared to the pre-alloyed high-alloy (CrM-0.5C) region. In the low-alloy region, higher secondary compaction pressure effectively reduce pores resulting in greater increase in hardness. However, the high-alloy region already exhibits higher hardness because of the cementite phase so that the contribution to the increase in hardness by pore removal due to the secondary compaction is relatively less significant. These variations of mechanical behavior are well agreed with the microstructure described in Fig. 3.

Figure 5 shows interfacial boundary region between high- and low-alloy in Fig. 5(a), and EDS elemental mapping of Cr and Cu, respectively in Fig. 5(b) and 5(c). In Fig. 5(a), the light gray region is high-alloy region, and the dark gray region is low-alloy region. The high-alloy (CrM-0.5C) and low-alloy (Fe-3Cu-0.5C) used in this research generally exhibit distinct sintering mechanisms. CrM generally shrinks during sintering because of the solid-phase sintering, however the liquid-phase

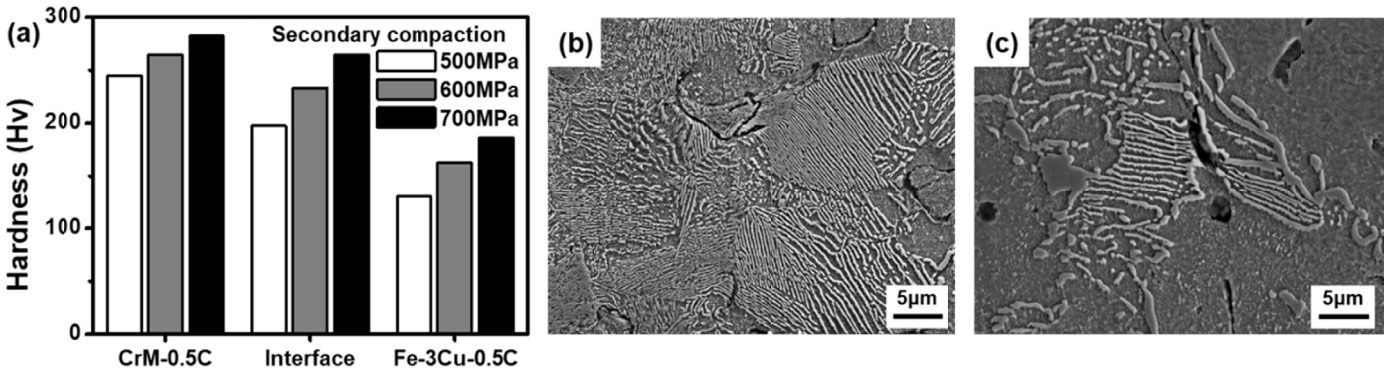

Fig. 4. (a) Hardness variation depending on the secondary compaction pressures in three different regions, and the microstructure of (b) high-alloy (CrM-0.5C) region and (c) low-alloy (Fe-3Cu-0.5C) region

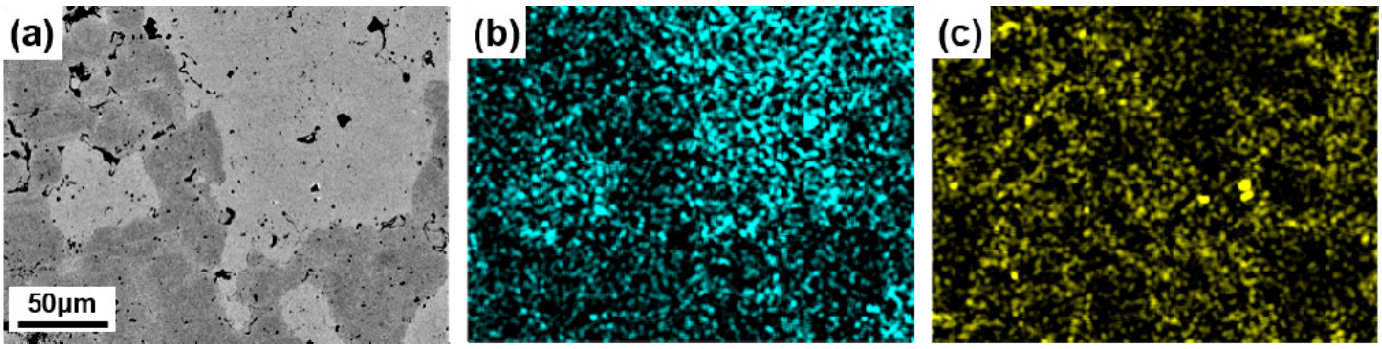

Fig. 5. (a) Microstructure of interfacial region between high- and low-alloys, and corresponding EDS elemental mappings of (b) Cr and (c) Cu ental mappings of (b) Cr and (c) Cu

sintering is dominated in Fe-Cu-C so that the volume tends to expand. By this reason, cracks or defects are likely to occur in the bonding interface. However, there are no cracks observed in the interfacial boundary between high- and low-alloys in this research. This can be explained by diffusion behavior of Cr and C. The Cr-rich phase was observed in high-alloy shown in Fig. 5(b), while Cu is found in virtually all regions as seen in Fig. 5(c). The Cu became a liquid phase during sintering process, and its fluidity is increased so that it is rapidly diffused along the powder and grain boundaries. So a large amount of Cu is also observed around the CrM powder. The Cu liquid phase serves as a brazing material to bond the powders each other on the interface boundary. Also, dissolution and re-precipitation of the Fe and CrM powders occur through this liquid phase leading to neck growth in a short time. Due to the inter-diffusion of these additive alloying elements, densification of the interface boundary was achieved successfully, and cracks were not formed during sintering process.

4. Conclusions

In this study, we proposed a novel method to produce hybrid P/M structure using dissimilar ferrous alloys consisting of a high-alloy (Astaloy® CrM®-0.5C) powder for high strength and a low-alloy (Fe-3Cu-0.5C) powder for high machinability. The mixed low-alloy powder was primarily compacted, and the pre-alloyed high-alloy powder was fed around the low-alloy compact. The hybrid structure was secondarily compacted using three different pressures (500, 600, 700 MPa). The hardness of high-alloy region was greater than that of low-alloy region, because Cr element in high-alloy forms resulting in a large amount of pearlite with very fine lamellar spacing, while Cu element in low-alloy forms a coarse ferrite during sintering. The high-alloy exhibits solid-phase sintering with volume contraction, while the low-alloy shows liquid-phase sintering with volume expansion. Although the high-alloy and low-alloy have different sintering mechanisms in terms of densification, cracks were not formed in the interfacial boundary. The alloying elements, Cr and Cu, are rapidly diffuses through the interface boundary, the densification of the boundary was achieved. Therefore, two different ferrous P/M alloys having distinct sintering and densification mechanisms were successfully consolidated without cracks or distortion.

Acknowledgments

This research was supported by Basic Science Research Program through the National Research Foundation of Korea (NRF) funded by the Ministry of Education (NRF-2018R1D1A1B07044481).

REFERENCES

[1] T. Jia, M. Militzer, ISIJ International **52**, 644 (2012).
[2] H. Chen, S. Zwaag, Philos. Mag. Lett. **86**, 92 (2012).
[3] H. Chen, S. Zwaag, Acta Mater. **61**, 1338 (2013).
[4] G. Purdy, J. Agren, A. Borgenstam, Y. Brechet, M. Enomoto, T. Furuhara, Metall. Mater. Trans. A, **42A**, 3703 (2011).
[5] W.T. Reynolds, S.K. Liu, F.Z. Li, S.S. Hartfield, H.I. Aronson, Metall. Trans. A, **21**, 1433 (1990).
[6] S. Liu, J. Hu, H. Wang, Opt. Laser Technol. **39**, 758 (2007).
[7] X. Dong, J. Hu, H. Wang, J. Mater. Process. Technol. **209**, 3776 (2009).
[8] R.M. Anklekar, K. Bauer, D.K. Agrawal, R. Roy, Powder Metall. **48**, 39 (2005).
[9] K.S. Narasimhan, Mater. Chem. Phys. **67**, 56 (2001).
[10] F. Nekatibeb, A.R. Annamalai, A, Upadhyaya, T. Indian I. Metals, **64**, 81 (2011).
[11] J. Capus, Met. Powder Rep. **66**, 11 (2011).
[12] J.L. Johnson, Int. J. Refract. Metals. Hard Mater. **53**, 80 (2016).
[13] M. Jeandin, J.L. Koutny, Y. Bienvenu, Powder Metall. **26**, 1 (1983).
[14] R.M. German, P. Suri, S.J. Park, J. Mater. Sci. **44**, 1 (2009).
[15] J. Park, G. Jeong, S. Kang, S. Lee, H. Choi, Met. Mater. Int. **21**, 1031 (2015).
[16] E. Lichanska, M. Sulowski, A. Cias, Arch. Metall. Mater. **61**, 109 (2016).
[17] H.I. Aaronson, W.T. Reynolds, G.R. Purdy, Metall. Mater. Trans. A, **37A**, 1731 (2006).
[18] G.R. Purdy, Scripta Mater. **47**, 181 (2002).
[19] Z.G. Yang, H.S. Fang, Curr. Opin. Solid State Mater. Sci. **9**, 277 (2005).